Digital Object Identifier: 10.1109/ULTSYM.2008.0149

Initial Growth and Coalescence of Acoustically Vaporized Perfluorocarbon Microdroplets

Kevin J. Haworth and Oliver D. Kripfgans
Department of Radiology and the Applied Physics Program
University of Michigan
Ann Arbor, USA
khaworth@umich.edu

***Abstract*—Acoustic droplet vaporization (ADV) is a technique whereby liquid droplets are vaporized into gas bubbles using ultrasound. This process and the resulting bubbles have been proposed for embolization, drug delivery, aberration correction, and bubble-enhanced high intensity focused ultrasound. To increase the efficacy of these applications, high-speed photography was used to study the initial phase-transition process. One-hundred and seven albumin-stabilized dodecafluoropentane droplets with diameters ranging from 3 to 20 µm were vaporized in a 100 µm inner-diameter polyethylene tube. Sixteen optical full-frame images and an optical streak image were obtained to record the vaporization, using a water immersion microscope (12 pixels per micron resolution). Framing rates were up to 13 MHz and streak speeds were up to 64 lines per microsecond. First, the impact of two- versus thirteen-cycle vaporization pulses was analyzed. It was found that with a two-cycle vaporization pulse only a portion of the droplet phase transitioned, whereas with a thirteen-cycle vaporization pulse the entire droplet phase transitioned. Using thirteen-cycle vaporization pulses, it was then observed that the bubbles all grew to approximately the same diameter within the first 2 µs. It was additionally observed that as neighboring bubbles grew in the first 15 µs, they could coalesce.**

Keywords - acoustic droplet vaporization; high-speed photography

I. INTRODUCTION

In 1998, Apfel proposed using ultrasound, among other sources, to phase-transition superheated liquid droplets for biomedical applications, a process known as acoustic droplet vaporization (ADV) [1]. Since then, the ADV process has been studied, as have its applications, including occlusion therapy [2],[3] and aberration correction [4]. It has additionally been proposed that ADV can be used as a drug delivery technique and as a method to produce gas bubbles for bubble-enhanced high-intensity focused ultrasound. Each of these techniques can benefit from specific pathways for ADV. For instance, it has been observed that depending on the acoustic and fluid parameters, ADV can occur with and without inertial cavitation [5]. For drug delivery, inertial cavitation may be a useful means of actively assisting drugs, incorporated into the droplets, to cross vascular or cellular membranes when the droplets vaporize. For occlusion therapy, the vessel rupture that can be associated with inertial cavitation may make it more difficult to occlude flow. For aberration correction, it is desirable to produce a small, isolated, single bubble, whereas bubble-enhanced high-intensity focused ultrasound may benefit from a higher density of bubbles as might be achieved with fragmentation. For this reason, it is important to fully understand the pathways associated with the formation of gas bubbles using ADV.

To investigate these pathways, high-speed photography was used to study up to the first sixteen microseconds of the vaporization process. Initially, the impact of the acoustic pulse length was observed. Next, the growth of the bubble over the first two microseconds was monitored. Finally, the coalescence of two bubbles near each other was recorded. This article will describe the experimental setup used to make these observations, the results of these observations, and finally a discussion of future areas of study.

II. EXPERIMENTAL SETUP

The experimental setup can be seen in fig. 1.

A. Droplet Preparation

ADV droplets were manufactured by first creating a solution of 4 mg per mL bovine albumin (A3803, Sigma-Aldrich, St. Louis, MO, USA) in normal saline (0.9% w/v, Hospira Inc., Lake Forest, IL, USA). 750 µL of this solution was added to a 2 mL glass vial. Then liquid dodecafluoropentane (DDFP, L16969, Alfa Aesar, Ward Hill, MA) was added gravimetrically to a final DDFP volume fraction of 25%. The vial was capped and shaken for 45 seconds at 4550 cycles per minute using an amalgamator (VialMix, Lantheus Medical Imaging, Billerica, MA, USA). The droplets were then refrigerated (5°C) until use.

B. Imaging Specifications

Full frame photography was performed using a Specialised Imaging Multi-Channel Framing Camera (SIM802, Specialised Imaging Ltd., Hertfordshire, UK). Sixteen full frame images (1360 x 1024 pixels) could be obtained with a frame rate of up to 200 MHz. Coupled to the SIM802 was a streak camera (Optoscope SC-10, Optronis GmbH, Kehl, Germany) capable of simultaneously obtaining streak speeds up to 64 lines per microsecond. Illumination was provided with a 300 Joule, 12 µs flash lamp.

Work supported in part by NIH Grants 5R33CA112144-02, 5R33 CA112144-02 and R21CA116043-01, and the Rackham Graduate School at the University of Michigan

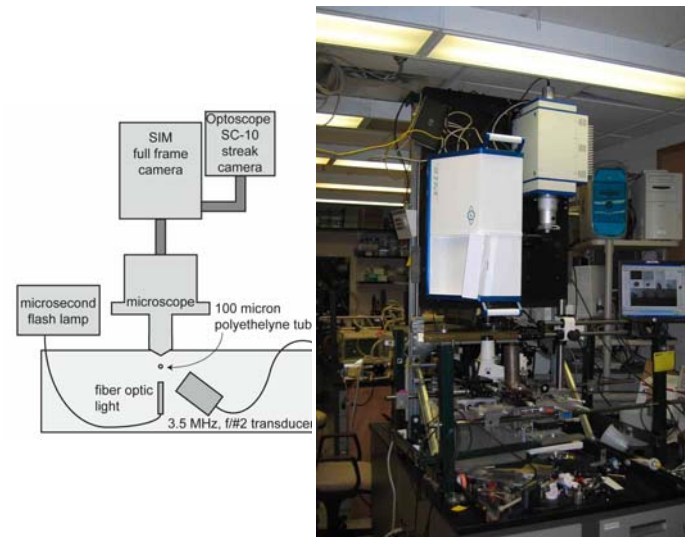

Figure 1. Experimental setup of the ultra high-speed imaging system (schematic on left, photo on right). The full frame camera is coupled to the streak camera on a vertical optical table. Below is a hybrid microscope with a 40x water immersion long distance objective. Droplets are positioned in the acoustic and optical field using a polyethylene tube (shown in cross-section).

Magnification was achieved by placing a 50 mm to 24 mm Nikkor lens (Nikon Inc., Melville, NY, USA) on the camera to provide a two-times gain. The Nikkor lens was focused on the camera port of a Nikon eclipse series microscope with a forty-times water objective. The cumulative magnification resulted in a 12 pixels per micron resolution for the full frame images (corresponding to a 113 by 85 micron field of view).

C. *Acoustics*

Confocal with the 40 times water objective was a 3.5 MHz, f/#2 single-element transducer with a focal distance of 38.1 mm (A381S, Panametrics, Olympus NDT Inc., Waltham, MA, USA). A function generator (33120A, Agilent, Palo Alto, CA, USA) was gated with a secondary function generator (3314A, Agilent) to produce single two, six, or thirteen-cycle tone bursts. The tone bursts were amplified with a power amplifier (Model 350, Matec, Northborough, MA, USA). The amplified signal was transmitted to the transducer. The acoustic output was measured to be 8 MPa (peak rarefactional) in a water path. ADV droplets were brought to the focus via a 100 micron inner-diameter polyethylene tubing. The tube was oriented to be perpendicular to the optical and acoustic beams. The entire setup was contained within a water tank at 22°C. Note that at this temperature the DDFP is not superheated.

III. RESULTS

A. *Acoustic Pulse Duration*

Three burst lengths were initially investigated using interframe times of 1.025 μs and exposures of 25 ns. Thirteen vaporization events were observed with an approximately two-cycle tone burst, seven events for an approximately six-cycle tone burst, and fifteen events for an approximately thirteen-cycle tone burst. The droplets varied between six and twenty microns in diameter for the two-cycle tone bursts and between 4.5 and 15 microns for the thirteen-cycle tone bursts. Fig. 2 shows typical results for the two and thirteen-cycle tone bursts.

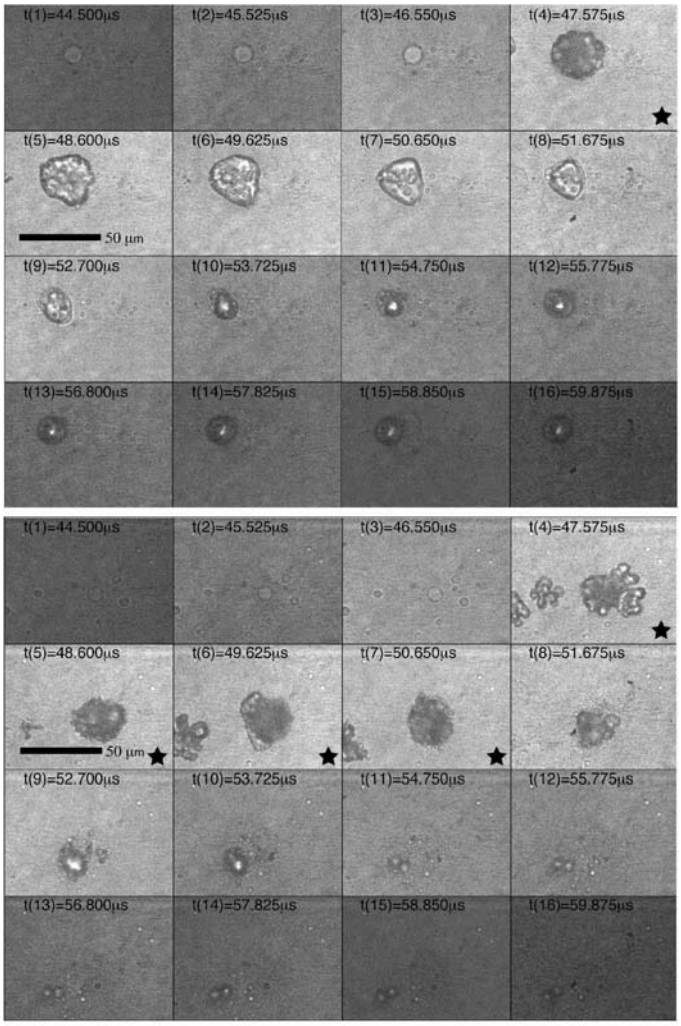

Figure 2. Sixteen image sets showing vaporization using approximately two-cycle tone bursts (top) and thirteen-cycle tone bursts (bottom). The presence of ultrasound during a frame is denoted by a star. The timing of the frames is seen in the upper left of each frame. The key difference between the two conditions is that not all of the DDFP phase-transitions when only a two-cycle tone burst was used. Note that the differences in intensities between frames is a result of the duration of the flashlamp.

The most striking difference is that for the two-cycle case, it is seen that not all of the DDFP phase-transitioned to a gas. This result was seen in all cases and for all droplet sizes tested. In comparison, for the thirteen-cycle tone burst, the images seem to show all of the DDFP phase transitioning during the on-time of the acoustics. This result was seen in all fifteen cases tested. For the six-cycle tone burst, incomplete vaporization was observed for three cases, and all of the DDFP phase-transitioned for the other four cases.

Another interesting observation is that for the two-cycle cases, the shell appears to have remained intact. This is seen in the clear and sharp delineation of the edge of the droplet and the lack of fragmentation (fig. 2 top). It is possible that these observations are not due to the shell but instead the result of the

immiscible nature of DDFP in water. Further work with fluorescent shells or another marker is needed to fully elucidate this point.

Based on the result of this section, all of the following experiments were performed using thirteen-cycle tone bursts to ensure complete vaporization.

B. Initial Vaporization Dynamics

The initial vaporization dynamics were studied next by using 75 ns interframe times (13 MHz frame rates) and 25 ns exposures. Due to the short interframe time, once the ultrasound arrives, it remains present for the remainder of the frames. Thirty-seven vaporization events were studied in this manner. Fig. 3 shows an example vaporization event.

The first point to note is that the effect of the compressional and rarefactional portions of the wave can been seen in the oscillatory nature of the transitioning bubble. This is possible because the interframe time is approximately one-quarter of an acoustic period at 3.5 MHz. The effect is most obvious in frames six and seven, where one sees the nucleation bubble appear and then disappear, respectively. In frame eight the bubble again returns. The oscillation effect can be seen again going from frames ten to thirteen where the growth of the bubble seems to slow and perhaps decrease slightly before again continuing to grow more quickly.

To study this effect more concretely, the droplet/bubble radius as a function of time since nucleation was determined for all thirty-seven vaporization events. Fig. 4 plots the bubble radius versus elapsed time. Due to the varying size of each initial droplet, and changes in relative position due to tube movement and droplet position within the tube, there is a relatively large variance between each droplet. However, it is clearly seen that the oscillatory nature is present in most of the vaporization events.

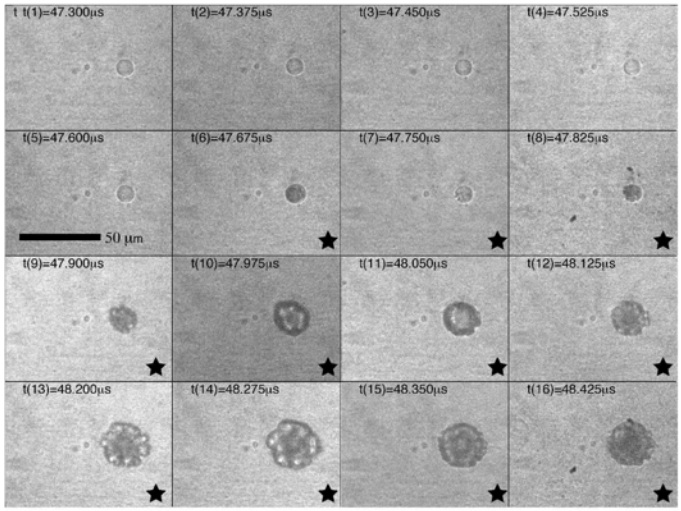

Figure 3. Example vaporization event imaged with a 75 ns interframe time. The stars indicate when the acoustic pulse is present. Note that the effects of the compressional and rarefactional portion of the waves can be seen in the oscillatory nature of the transitioning bubble.

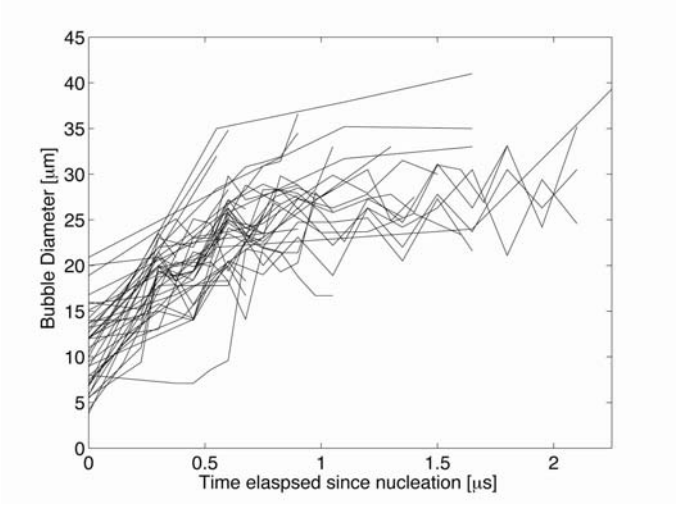

Figure 4. The bubble diameter versus time since nucleation for all thirty-seven vaporization events analyzed. Note that the oscillation in droplet diameter with the acoustic period is evident in most of the vaporization events. The diameter at time zero is the initial droplet diameter.

Another feature that begins to become apparent from fig. 4 is that the bubble diameter after one to two microseconds is independent of the initial droplet diameter. Fig. 5 shows the maximum bubble diameter during the first two microseconds as a function of the initial droplet diameter. A linear fit shows a nearly flat slope. The squared correlation coefficient (r^2) is 0.012, indicating a lack of correlation between the initial droplet diameter and the maximum bubble diameter. Clearly during the first two microseconds, the bubble has not reached its terminal size. However, the results indicate that the initial bubble grows independent of the size of the droplet. This likely indicates that the initial bubble growth is driven by acoustics and/or the consumption of DDFP with all the tested droplets not phase-transitioning all of the DDFP during the first two microseconds.

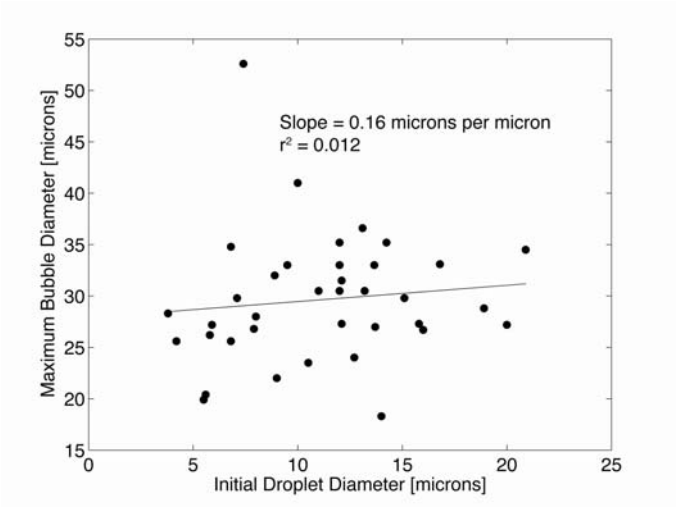

Figure 5. The maximum bubble diameter achieved during the first two microseconds versus the droplet diameter that produced the bubbles.

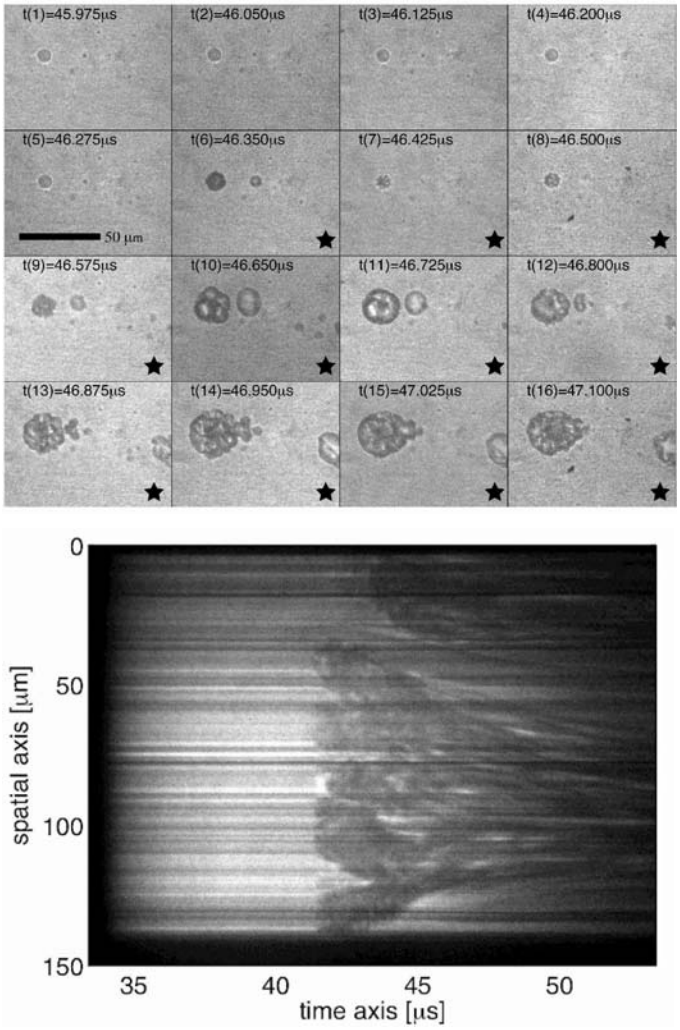

Figure 6. (Top) Example full frame images showing the coalescence of two bubbles that vaporized near each other. The coalescence is not the result of the two bubbles expanding into each other, but the center of mass of the smaller droplet moving towards the larger bubble. (Bottom) The streak image shows many droplets vaporizing near each other and coalescing. Note that the coaclescence continues to occur beyond the one microsecond seen in the full frame images

C. Bubble Coalescence

In the process of vaporization, it was seen in 35 cases (not used in the previous analysis), that when two or more droplets vaporized near each other, they would coalesce. The coalescence was not the result of bubbles growing into each other, but rather the centers of mass moving towards each other. This occurred while the acoustics were on. It is believed that the coalescence is due to secondary Bjerknes radiation force. Measuring the relative velocity, it was found that the average droplet-droplet impact velocity was 9 m/s and that the impact velocity varied between 4.5 and 16.5 m/s

IV. CONCLUSIONS

It has been seen that the acoustic pulse length has a significant impact on the initial vaporization process. With two-cycle tone bursts, it was seen that part of the DDFP did not vaporize and it is possible that the shell remained intact. The isolated bubble that would result from this could be beneficial for producing point-targets for phase aberration correction. If in fact the shell remains intact however, this would have a very detrimental impact on the ability to deliver drugs. For thirteen-cycle tone bursts, it was seen that all of the DDFP phase transitioned. In this process, fragmentation could also be seen. The fragmentation may be beneficial in distributing drugs and producing multiple bubbles for bubble-enhanced high-intensity focused ultrasound thermal therapy.

Using thirteen-cycle tone bursts, the initial vaporization process was studied and it was found that the maximum bubble diameter during the first two microseconds was independent of the size of the droplet that the bubble originated from. This may indicate that small droplets have a faster wall velocity as they vaporize. If this is the case, then the acoustic emission from a small versus large droplet might be able to be isolated, allowing for an *in vivo* assessment of the size droplets being vaporized. This knowledge would be useful for all of the applications discussed.

Finally, it was seen that droplets near each other could coalesce. This coalescence may be highly beneficial for occlusion therapies, as large bubbles will occlude higher in the vascular tree. The coalescence may be detrimental to aberration correction however if the bubble is too large to be considered a point target. The coalescence may also impact how drugs are distributed upon vaporization.

The results of this work suggest additional data be obtained to further elucidate the points highlighted here. It is also important that the work here be repeated in a water bath at 37^{o}C to simulate the impact of superheat, which would be experienced *in vivo*.

REFERENCES

[1] R.E. Apfel, "Activatable infusible dispersions containing drops of a superheated liquid for methods of therapy and diagnosis," U.S. Patent 5840276, 1998.

[2] O.D. Kripfgans, J.B. Fowlkes, M. Woydt, O.P. Eldevik, and P.L. Carson, "In vivo droplet vaporization for occlusion therapy and phase aberration correction," IEEE Trans. Ultrason. Ferroelec. Freq. Contr., vol. 49, no. 6, pp. 726-738, 2002.

[3] O.D. Kripfgans, C.M. Orifici, P.L. Carson, K.A. Ives, O.P. Eldevik, and J.B. Fowlkes, "Acoustic droplet vaporization for temporal and spatial control of tissue occlusion: a kidney study," IEEE Trans. Ultrason. Ferroelec. Freq. Contr., vol. 52, no. 7, pp. 1101-1110, 2005.

[4] K.J. Haworth, J.B. Fowlkes, P.L. Carson, and O.D. Kripfgans, "Towards aberration correction of transcranial ultrasound using acoustic droplet vaporization," *Ultrasound Med. Biol.,* vol. 34, no. 3, pp. 435-445, 2008.

[5] M.L. Fabiilli, K.J. Haworth, N.H. Fakhri, O.D. Kripfgans, P.L. Carson, J.B. Fowlkes, "The Role of Intertial Cavitation in Acoustic Droplet Vaporization," IEEE Trans. Ultrason. Ferroelec. Freq. Contr., submitted